Journal of Renewable Materials

Tech Science Press

DOI: 10.32604/jrm.2021.013664

ARTICLE

# Analysis on Pore Structure of Non-Dispersible Underwater Concrete in Saline Soil Area

**Fang Liu[1], Baomin Wang[2,*], Mengsai Wang[2] and Xiaosa Yuan[1]**

[1]Shaanxi Key Laboratory of Safety and Durability of Concrete Structures, Xijing University, Xi'an, 710123, China

[2]School of Civil Engineering, Dalian University of Technology, Dalian, 116023, China

[*]Corresponding Author: Baomin Wang. Email: wangbm@dlut.edu.cn

Received: 16 August 2020 Accepted: 16 October 2020

**ABSTRACT**

In this paper, mercury intrusion porosimetry (MIP) is used to test the pore structure of non-dispersible underwater concrete so as to study the influence of pouring and curing environment, age and slag powder on the pore characteristics of concrete, analyze the pore characteristics, porosity and pore distribution of concrete in different hydration stages, and reveal the relationship between pore structure and permeability of concrete. The results show that the pore-size distribution of concrete in fresh water condition is better than that in sulfate environment and mixed salt environment, and therefore, sulfate as well as mixed salt are not conducive to the development of pore structure of non-dispersible underwater concrete; chlorine salt has little effect on the pore structure of non-dispersible underwater concrete; under the three conditions of sulfate, chlorine and mixed salt, the porosity of concrete mixed with slag powder is lower than that of concrete without slag powder. The results indicate that the addition of slag powder can ameliorate the pore size distribution of non-dispersed underwater concrete, reduce the porosity, and make the concrete structure more compact, which is beneficial to improve the permeability resistance of concrete at the macro level.

**KEYWORDS**

Non-dispersible underwater concrete; slag powder; saline soil; mercury intrusion porosimetry (mip); pore structure

## 1 Introduction

With the continuous exploitation and utilization of water resources, underwater projects such as sea crossing bridges, wharves and dams have become more and more common [1,2]. There is always the problem of pouring concrete in underwater engineering. The traditional method of underwater pouring concrete is to pour concrete under the condition of water isolation, or to use the conduit with good sealing property to directly inject the concrete into the appropriate position for construction [3]. However, there are multiple defects in these traditional construction methods, like environmental pollution, prolonged construction period, increased project costs, and the higher requirements on technology and construction equipment, etc.

Directly pouring concrete under water can omit the step of isolating water, thereby saving costs and shortening the construction period. However, ordinary concrete cannot be used in engineering because it will be scoured by the currents in the process of concreting, resulting in the separation of cement slurry

and aggregate, which severely affects the cementation ability and causes excessive loss of concrete strength [4]. In order to solve some problems in the practical application of underwater concrete, some scholars have studied and designed the underwater materials [5,6].

The biggest difference between non-dispersible underwater concrete and ordinary concrete is that a water-soluble polymer compound is added to the former as the dispersion resistance agent [7]. This kind of anti-dispersion agent has the ability to bond the cement paste more firmly. Even if washed by water, the cement paste can still stick to the aggregate and sink to the bottom without dispersing, which avoids dispersion and segregation of concrete [8], so it has less environmental pollution [9,10] as well as less strength loss [11]. Grzeszczyk [12] investigates the effect of $SiO_2$ nanoparticles on the washout of underwater concrete, which shows an improvement of resistance to washout. Various viscosity modifiers admixtures are used as anti-washout admixtures (AWAs) to fabricate non-dispersible underwater concrete [13], and the results indicate that the gum Arabic, super absorbent polymer, and Xanthan gum are most suitable AWAs for non-dispersible underwater concrete.

Mainly distributing in arid and semi-arid inland regions and some parts of coastal areas, saline soil contains a large number of ions with strong corrosion such as $SO_4^{2-}$, $Cl^-$ and $Mg^{2+}$ [14] which are much more than that in seawater [15,16], and seriously corrode buildings [17–21]. For concrete structures, the most harmful ones in saline soil are sulfate and chlorine [22,23]. Because sulfate will invade into the concrete to form crystals and expand, resulting in concrete cracking and concrete structure damage [24]; chlorine in the concrete will slowly permeate to the steel bar, and then destroy the passivation layer of the steel bar after reaching a certain concentration, which will bring about the corrosion of reinforcement and the reduction of its bearing capacity [25–27].

Good impermeability can slow down the diffusion speed of $SO_4^{2-}$, $Cl^-$ and other ions in concrete, delay the expansion and cracking of concrete and corrosion of steel bars, thereby increasing the service life of concrete structures. Impermeability is an important index to measure the durability of concrete, so it is of great significance to study the impermeability of concrete in saline soil.

The article aims in studying the impermeability of non-dispersible underwater concrete in saline soil area by the means of microscopic analysis of concrete pore structure. In the simulated saline soil environment, concrete is poured and cured under water, and compared with that under fresh water environment. The difference of pore structure of non-dispersible underwater concrete at different ages and the influence of diverse erosion environment on the pore structure of concrete are detected by using MIP test. In addition, the influence of slag powder on the pore structure of non-dispersible underwater concrete is investigated. Through the analysis of the pore structure of non-dispersible underwater concrete, the main factors affecting the development of concrete pores are found out, and the influence on the impermeability of non-dispersible underwater concrete is discussed.

## 2 Experimental

### *2.1 Raw Materials*

The P·O 42.5R cement produced by Dalian Onoda Cement Co., Ltd., China, was used in this test. The specific performance indexes are shown in Tabs. 1 and 2.

The fine aggregate used in this experiment was natural river sand with a fineness modulus of 2.8. The coarse aggregate was continuous graded limestone with size of 5–20 mm and apparent density of 2740 kg/m$^3$. Anti-dispersion agent was UWB-II flocculant produced by Research Institute of China Petroleum Engineering, whose main ingredient was water-soluble carbohydrate polymers. The mineral admixture was ground granulated blast-furnace slag (GGBS, S105 grade) made by Shandong Luxin New Building Materials Co., Ltd., and its specific composition is shown in Tab. 3. The water for mixing

concrete in this experiment was the tap water provided by laboratory. The water reducing agent was manufactured by Dalian Bonuo Biochemical Reagent Factory, and its type was polycarboxylic superplasticizer.

**Table 1:** Cement performance index

| Specific surface area ($m^2$/kg) | Setting time (min) | | Ignition Loss (%) | Strength at 3d (MPa) | | Strength at 7d (MPa) | | Strength at 28 d (MPa) | |
|---|---|---|---|---|---|---|---|---|---|
| | Initial setting | Final setting | | Flexural strength | Compressive strength | Flexural strength | Compressive strength | Flexural strength | Compressive strength |
| 330 | 227 | 282 | 3.61 | 4.6 | 21.2 | 6.8 | 35.0 | 7.6 | 44.8 |

**Table 2:** Chemical composition of cement (%)

| CaO | $SiO_2$ | $Al_2O_3$ | $Fe_2O_3$ | $SO_3$ | MgO | $Na_2O$ | $K_2O$ |
|---|---|---|---|---|---|---|---|
| 61.16 | 21.49 | 5.24 | 2.89 | 2.53 | 2.12 | 0.76 | 0.42 |

**Table 3:** Chemical composition of GGBS (%)

| CaO | $SiO_2$ | $Al_2O_3$ | MgO | $SO_3$ | $TiO_2$ | $K_2O$ | MnO | $Fe_2O_3$ | $Na_2O_3$ |
|---|---|---|---|---|---|---|---|---|---|
| 40.075 | 30.311 | 14.991 | 8.595 | 3.219 | 0.839 | 0.501 | 0.399 | 0.388 | 0.324 |

### *2.2 Mixing Ratio of Concrete and Sample Preparation*

The mixing ratio of non-dispersible underwater concrete used in the test is illustrated in Tab. 4, where '0.45' in the number indicates the water-binder ratio of the non-dispersible underwater concrete, '0' means concrete without slag powder, and 'SL' signifies that the dosage of slag powder in the concrete is 60%.

**Table 4:** Mixing ratio of underwater non-dispersible concrete

| No. | water-binder ratio | Water (kg) | Binding material (kg) | Cement (kg) | Slag powder | | Fine aggregate (kg) | Coarse aggregate (kg) | Water reducer (%) | Flocculant (%) |
|---|---|---|---|---|---|---|---|---|---|---|
| | | | | | Mass (kg) | Replacement rate (%) | | | | |
| 0.45-0 | 0.45 | 200 | 445 | 445 | 0 | 0 | 690 | 1035 | 0.5 | 2.8 |
| 0.45-SL | 0.45 | 200 | 445 | 178 | 267 | 60 | 690 | 1035 | 0.5 | 2.8 |

In accordance with Chinese Standard DL/T 5117-2000 [28], the preparation process of non-dispersible underwater concrete is as follows:

a) First, the mold was put into the water tank, and fresh water or salt solution was added into it to 150 mm above the top of the mold, and then the concrete mixture was slowly poured from the water surface to ensure the mixture fall freely into the mold in the water. The amount of the mixture to be poured each time was about one tenth of the mold capacity.

b) The casted mold was taken out from the water and placed at a flat place for 5 min to make the concrete self-leveling, then both sides of the mold were gently knocked by a wooden hammer in order to drain the surplus water out of the mold.

c) The concrete mixture higher than the mold was lightly scraped with a spatula until the surface was flat and the height was level with the mold. After the mixture sticking to the outside of the mold was cleaned up, the mold was put into fresh water or salt solution again.

d) 48 hours later, the mold was gently dismantled. Finally, the concrete specimens were put back into fresh water or salt solution for continuous soaking and curing, and a certain distance should be kept between the specimens. The optimum curing temperature for specimens was 20°C~25°C.

### *2.3 Preparation of Erosion Solution*

In this experiment, the process of underwater concrete pouring in saline soil environment was simulated, and then the concrete specimens were immersed in salt solution for erosion. The erosion solutions selected in this study were divided into three types: The chlorine solution with $Cl^-$ concentration of 50000 mg/L, the sulfate solution with $SO_4^{2-}$ concentration of 20000 mg/L, as well as the mixed solution of chloride and sulfate in which the concentration of $Cl^-$ and $SO_4^{2-}$ was 50000 mg/L and 20000 mg/L respectively. The salt solution was made of industrial-grade sodium sulfate and sodium chloride, and was replaced every 15 days during the immersion and erosion of the concrete specimens.

### *2.4 Test Method*

In this experiment, the pore characteristics of non-dispersible underwater concrete were measured by mercury intrusion porosimetry (MIP). The instrument used in the test was the automated mercury porosimeter, whose type is Micromeritics' AutoPore IV9500 Series, manufactured by Micromeritics Instrument Corp., USA.

The automated mercury porosimeter used in this test is shown in Fig. 1.


**Figure 1:** Automated Mercury Porosimeter

The process of sampling concrete in MIP test is as follows:

a) After curing to the set age, the specimens of non-dispersible underwater concrete were removed from the curing solution and fragmented, then the concrete fragments were put into the plastic bottle which was poured with anhydrous ethanol until the samples were submerged, in order to stop the hydration process of cement in concrete;
b) Before the test, the samples were taken out of the plastic bottle, smashed to particles with the diameter of 3~5 mm, the aggregates in the samples were removed, and about 10 g samples were selected for drying;
c) Then, the selected samples were put into an oven. It is better to use a vacuum oven with the temperature set at 150°C to create a vacuum environment. And then the samples were dried for one hour. Before opening the door of the oven, dry nitrogen was recharged, and then the samples were taken out and put into a sealed bag to avoid contact with air.

## 3 Results and Discussion

### *3.1 Analysis of Pore Structure Characteristics of Concrete in Sulfate Environment*

#### *3.1.1 Effect of Sulfate Environment on Pore Structure of Non-Dispersible Underwater Concrete*

The pore size distribution of concrete under sulfate attack and blank sample in fresh water at 28 d and 180 d is respectively shown in Figs. 2 and 3, where 'W' represents fresh water environment and 'SY' represents sulfate environment.

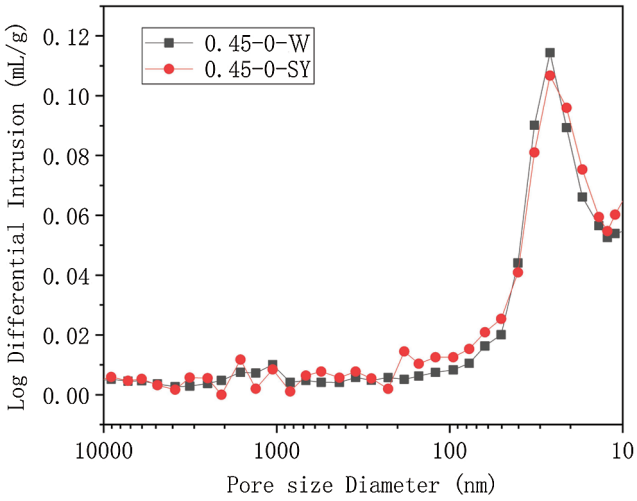


**Figure 2:** Log differential intrusion of concrete at 28 d

It can be seen from Fig. 2 that the pore size distribution trend of concrete in sulfate environment is roughly the same as that of blank sample. With the decrease of pore size, the mercury inflow gradually increases, indicating that the proportion of this pore size increases. The peak value of differential mercury intrusion curve is the most probable aperture, that is, the pore size with the highest probability of occurrence. The most probable aperture of the blank sample and concrete in sulfate environment is 28.29 nm and 27.28 nm respectively. The mercury intrusion amount of them is 0.114 ml/g and 0.106 ml/g respectively, with a difference of 7.5%, which illustrate that there is no significant difference in pore size between concrete in sulfate environment and that in fresh water environment at 28 d. In Fig. 3, when the concrete age reaches 180 d, the most probable aperture of the blank sample is 40.31 nm,

and the amount of mercury intrusion is 0.116 ml/g, while the most probable aperture of concrete in sulfate environment is 40.32 nm, and the mercury intrusion amount is 0.160 ml/g. The most probable pore sizes of the two samples are basically identical, but the mercury intrusion amount of concrete in sulfate environment is increased by 37.9% compared with the blank sample, which also indicates the increase of the number of such pores.

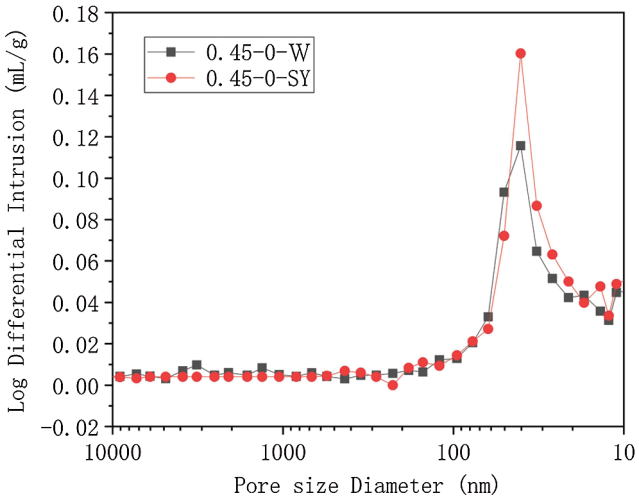


**Figure 3:** Log differential intrusion of concrete at 180 d

The cumulative pore area and mercury intrusion trend of concrete under sulfate environment and the blank sample at 28 d are shown in Fig. 4, and the trends of them at 180 d are shown in Fig. 5. The MIP analysis of non-dispersible underwater concrete in both sulfate environment and fresh water environment is shown in Tab. 5.

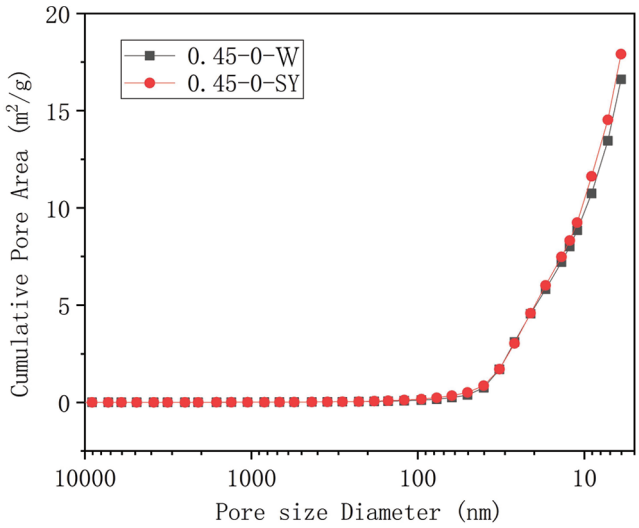


**Figure 4:** Cumulative pore area of concrete at 28 d

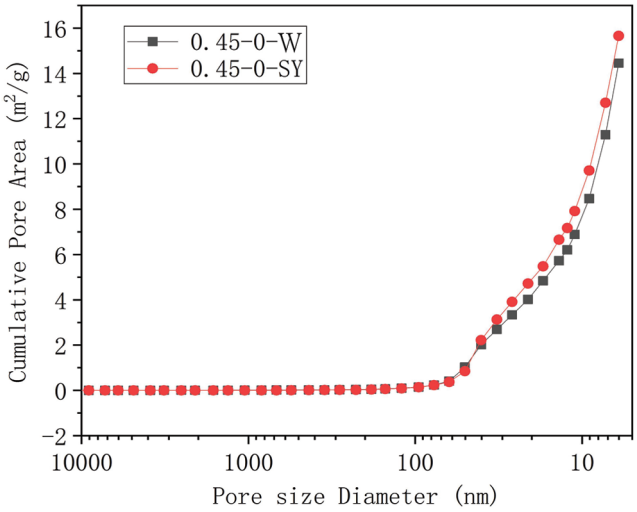


**Figure 5:** Cumulative pore area of concrete at 180 d

**Table 5:** MIP analysis of non-dispersible underwater concrete

| Sample | Age | Total intrusion volume (mL/g) | Median volume pore diameter (nm) | Median area pore diameter (nm) | Average pore diameter (nm) | Porosity (%) |
|---|---|---|---|---|---|---|
| 0.45-0-W | 28 d | 0.0918 | 29.1 | 11.8 | 21.5 | 20.04 |
| 0.45-0-SY | 28 d | 0.0964 | 28.3 | 11.4 | 22.1 | 20.09 |
| 0.45-0-W | 180 d | 0.0876 | 31.1 | 10.5 | 20.2 | 18.46 |
| 0.45-0-SY | 180 d | 0.0897 | 30.7 | 11.2 | 20.9 | 18.65 |

It can be seen from Fig. 4 that the cumulative pore area of concrete in sulfate environment is basically the same as that in fresh water environment at the age of 28 d. From Fig. 5, at the age of 180 d, the cumulative pore area of concrete in the sulfate environment is higher than that in freshwater environment, and the number of harmful pores with pore size greater than 50 nm is also higher than that of concrete in fresh water. As can be seen from Tab. 5, the porosity of concrete at the age of 180 d is lower than that at the age of 28 d. The porosity of concrete in sulfate environment is 1.03% higher than that of blank sample at 180 d. It can be explained that with the increase of age, the porosity of non-dispersible underwater concrete gradually decreases, and the impermeability of concrete is gradually enhanced; the corrosion of sulfate solution will increase the porosity of concrete and the number of harmful pores, which eventually degrade the impermeability of concrete.

*3.1.2 Effect of Slag Powder on Pore Structure of Non-Dispersible Underwater Concrete*

In the environment of sulfate erosion, the pore size distribution of concrete with 60% slag powder and the blank sample at the age of 28 d is shown in Fig. 6, and that at the age of 180 d is shown in Fig. 7. From Fig. 6, it can be seen that the most probable aperture of concrete mixed with slag powder is 6.03 nm, and that of the blank sample is 27.28 nm at the age of 28 d. And Fig. 7 shows that the most probable aperture of the blank sample is 40.32 nm, and that of the concrete mixed with slag powder is 7.24 nm. In both cases, the most probable aperture of the concrete mixed with slag powder is smaller than that of the blank sample, which indicates that the addition of slag powder improves the pore size distribution of the non-dispersible underwater concrete, makes the concrete more compact, and increases the impermeability of concrete.

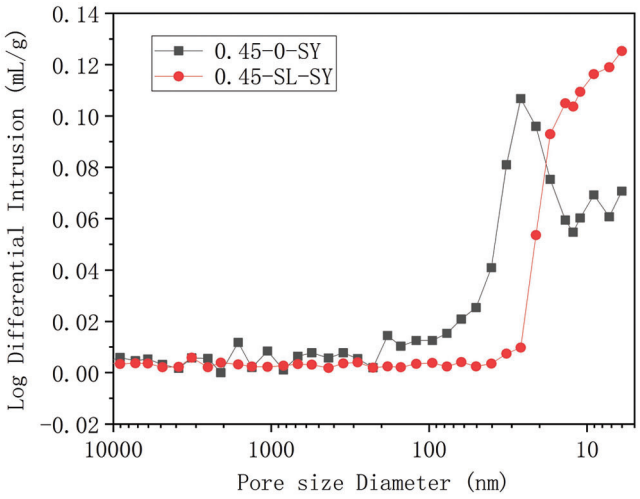


**Figure 6:** Log differential intrusion of concrete at 28 d

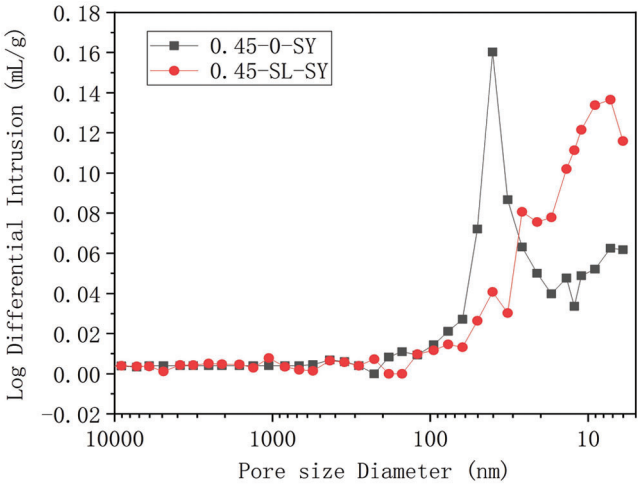


**Figure 7:** Log differential intrusion of concrete at 180 d

Fig. 8 shows the cumulative pore area and mercury intrusion trend of concrete mixed with 60% slag powder and the blank sample in sulfate environment at 28 d, and Fig. 9 represents that of trend at 180 d. MIP parameters of the blank sample and concrete with slag powder are shown in Tab. 6. It is clear from Fig. 8 that, at the age of 28 d, the cumulative pore area of concrete with slag powder is 24.507 $m^2/g$, which is higher than 17.913 $m^2/g$ of the blank sample; in addition, the number of harmful pores in concrete mixed with slag powder is lower than that of the blank sample. According to Fig. 9, when the pore size is smaller than 50 nm, the cumulative pore area of concrete mixed with slag powder is lower than that of the blank sample within certain range, verifying that the mixing of slag powder can reduce the number of harmful pores in concrete and improve the pore size distribution of concrete. As can be seen in Tab. 6, at the age of 180 d, the porosity of concrete mixed with slag powder is 12.82% lower than that of blank sample, which demonstrates that the addition of slag powder can reduce the porosity of non-dispersible underwater concrete, and enable the concrete structure more compact and impermeable.

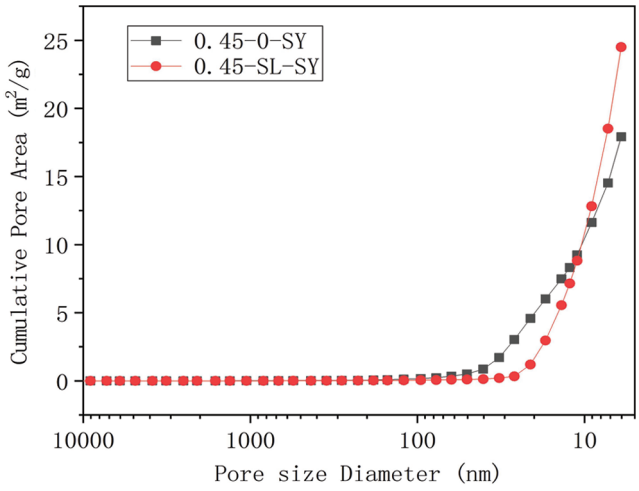


**Figure 8:** Cumulative pore area of concrete at 28 d

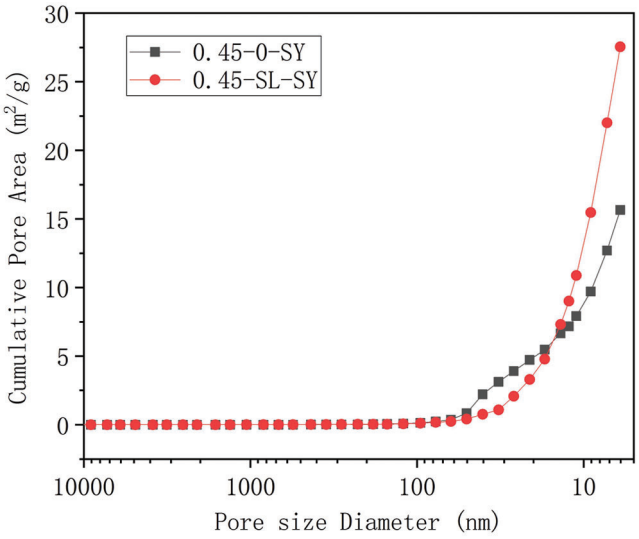


**Figure 9:** Cumulative pore area of concrete at 180 d

**Table 6:** MIP analysis of non-dispersible underwater concrete

| Sample | Age | Total intrusion volume (mL/g) | Median volume pore diameter (nm) | Median area pore diameter (nm) | Average pore diameter (nm) | Porosity (%) |
|---|---|---|---|---|---|---|
| 0.45-0-SY | 28 d | 0.0964 | 28.3 | 11.4 | 22.1 | 20.09 |
| 0.45-SL-SY | 28 d | 0.0881 | 24.5 | 9.3 | 21.4 | 19.77 |
| 0.45-0-SY | 180 d | 0.0897 | 30.7 | 11.2 | 20.9 | 18.65 |
| 0.45-SL-SY | 180 d | 0.0983 | 26.8 | 8.7 | 18.7 | 16.26 |

### *3.2 Analysis of Pore Structure Characteristics of Concrete in Chloride Environment*

#### *3.2.1 Effect of Chloride Environment on Pore Structure of Non-Dispersible Underwater Concrete*

Fig. 10 shows the pore size distribution of concrete in chloride environment and the blank sample in fresh water environment at 28 d, and Fig. 11 shows the distribution at the age of 180 d, where 'W' represents fresh water environment and 'LY' represents chloride environment.

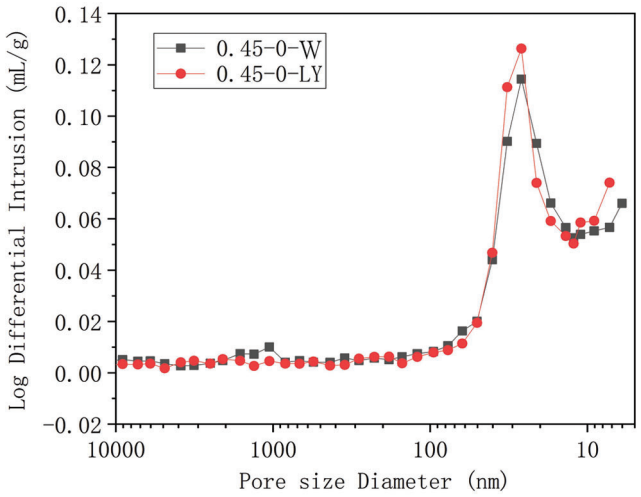


**Figure 10:** Log differential intrusion of concrete at 28 d

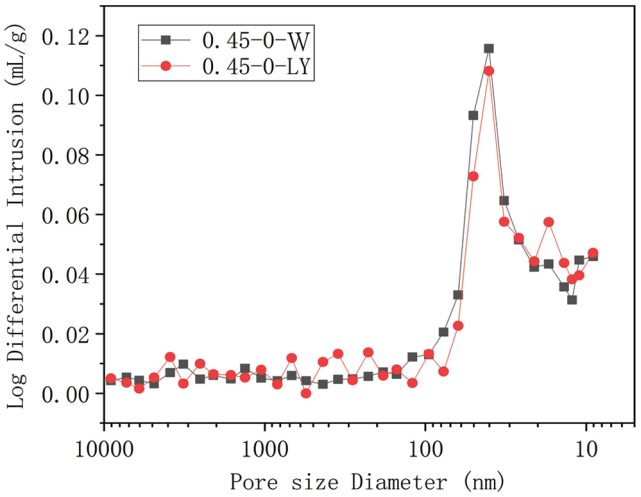


**Figure 11:** Log differential intrusion of concrete at 180 d

It can be seen from Figs. 10 and 11 that the pore size distribution trends of the two samples are essentially the same. In addition, the most probable aperture of concrete in the two environments is very similar, which indicates that chloride has no obvious effect on the pore structure of non-dispersible underwater concrete.

At the age of 28 d, the cumulative pore area and mercury intrusion trends of concrete in chloride environment and the blank sample in fresh water environment are presented in Fig. 12, which at 180 d

are shown in Fig. 13, and the MIP analysis of concrete in chloride environment and fresh water environment is given in Tab. 7.

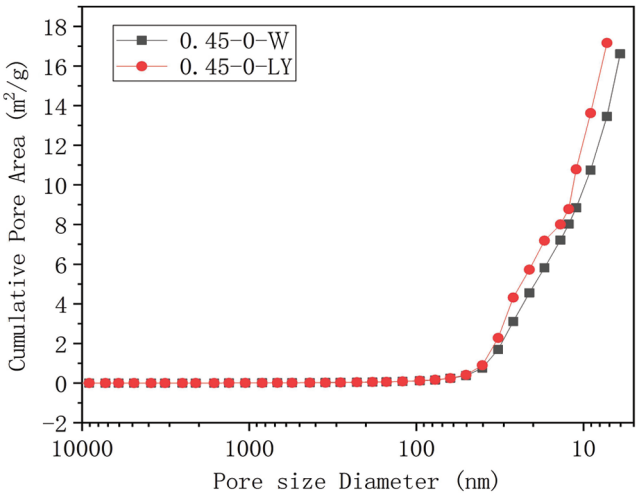


**Figure 12:** Cumulative pore area of concrete at 28 d

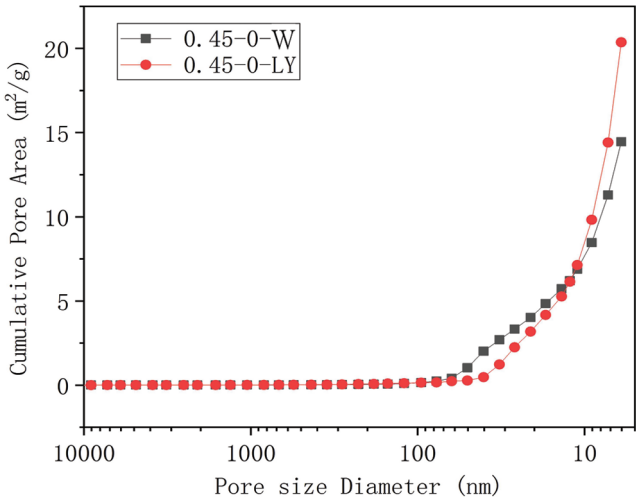


**Figure 13:** Cumulative pore area of concrete at 180 d

**Table 7:** MIP analysis of non-dispersible underwater concrete

| Sample | Age | Total intrusion volume (mL/g) | Median volume pore diameter (nm) | Median area pore diameter (nm) | Average pore diameter (nm) | Porosity (%) |
|---|---|---|---|---|---|---|
| 0.45-0-W | 28 d | 0.0918 | 29.1 | 11.8 | 21.5 | 20.04 |
| 0.45-0-LY | 28 d | 0.0855 | 28.7 | 11.3 | 19.9 | 19.29 |
| 0.45-0-W | 180 d | 0.0876 | 31.1 | 10.5 | 20.2 | 18.46 |
| 0.45-0-LY | 180 d | 0.0874 | 28.1 | 9.8 | 19.2 | 18.64 |

The curves in Fig. 12 clearly show that the cumulative pore area of concrete in fresh water environment is similar to that in chloride environment at the age of 28 d, which is 16.61 $m^2/g$ and 17.16 $m^2/g$ respectively, and the difference is only 3.3%. As seen in Fig. 13, the cumulative pore area of concrete in chloride environment is higher than that of the blank sample, and the content of harmful pores above 50 nm is less in both of them. Besides, the pore size distribution of concrete in chloride environment is slightly better than that of the blank sample. The data of Tab. 7 suggests that with the increase of age, the porosity of concrete gradually decreases, and the compactness of concrete increases gradually, which can enhance its impermeability on the macro level; the porosity of concrete in chloride environment is similar to that of blank sample. On the whole, the chloride environment has little effect on the pore structure of concrete, and thus does not have obvious influence on the impermeability of concrete.

*3.2.2 Effect of Slag Powder on Pore Structure of Non-Dispersible Underwater Concrete*

In chloride environment, the pore size distribution of concrete with 60% slag powder and the blank sample at 28 d is shown in Fig. 14, which at 180 d is shown in Fig. 15.

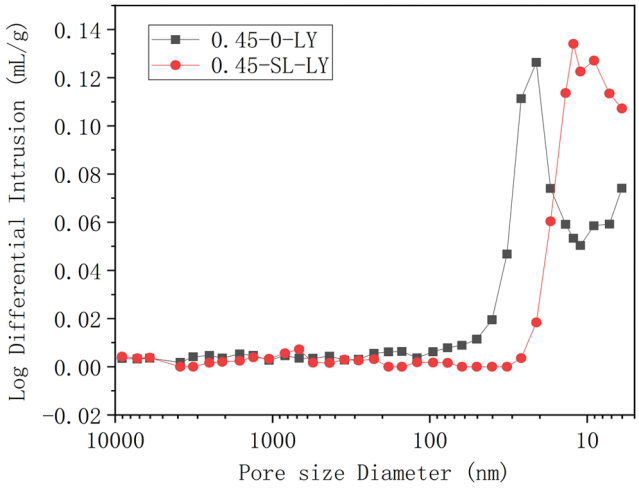


**Figure 14:** Log differential intrusion of concrete at 28 d

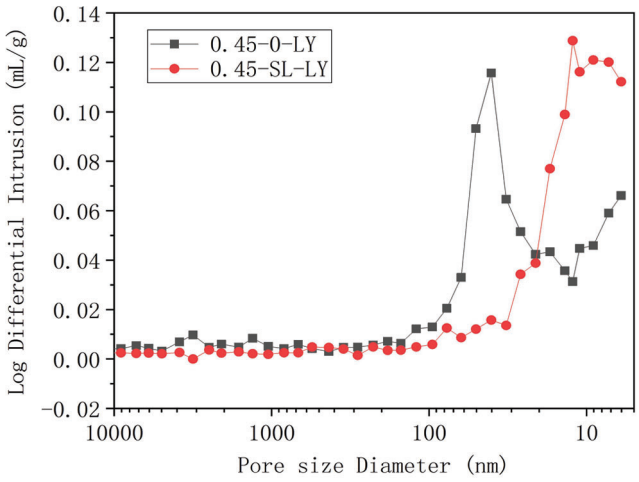


**Figure 15:** Log differential intrusion of concrete at 180 d

Fig. 14 represents that at the age of 28 d, the most probable aperture of concrete with slag powder and the blank sample is 12.24 nm and 21.09 nm respectively, and the content of mercury intrusion is 0.134 ml/g and 0.126 ml/g separately. The most probable aperture of concrete with slag powder is smaller than that of the blank sample. It can be seen from Fig. 15 that the most probable aperture of the blank sample is 40.32 nm at the age of 180 d, which is much larger than that of concrete with slag powder. The results prove that the pore size of non-dispersible underwater concrete mixed with slag powder is smaller, and the number of such pores is more, so the addition of slag powder can improve the pore size distribution of concrete to make concrete more compact, and enhance the impermeability of concrete on the macro level.

Fig. 16 presents the cumulative pore area and mercury intrusion trend of concrete with 60% slag powder and the blank sample in chloride environment at 28 d, and Fig. 17 displays the trend of cumulative pore area and mercury intrusion at 180 d age. The MIP analysis of the two samples is given in Tab. 8. According to Fig. 16, at the age of 28 d, the cumulative pore area of concrete mixed with slag powder differs little from that of blank sample-one is 18.074 $m^2/g$ and the other is 17.164 $m^2/g$; the cumulative pore area curve of concrete mixed with slag powder is below the curve of blank sample, and the number of harmful pores of the former is also lower than that of the latter. From Fig. 17, the number of pores with pore size over 50 nm in concrete mixed with slag powder is also less than that in blank sample, suggesting that the mixing of slag powder can reduce the number of harmful pores and improve the pore size distribution of concrete. Tab. 8 can represent that the porosity of concrete mixed with slag powder is 3.54% lower than that of blank sample at 180 d, which indicates that the porosity of non-dispersible underwater concrete can be reduced by adding slag powder.

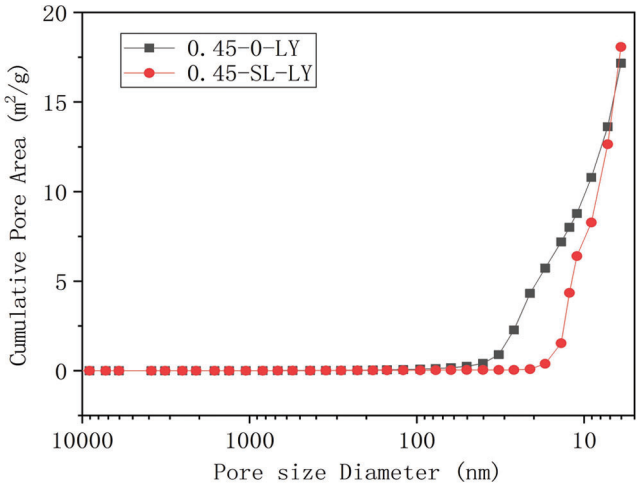


**Figure 16:** Cumulative pore area of concrete at 28 d

### *3.3 Analysis of Pore Structure Characteristics of Concrete in Mixed Salt Environment*

#### *3.3.1 Effect of Mixed Salt Environment on Pore Structure of Non-Dispersible Underwater Concrete*

The pore size distribution of concrete in mixed salt environment and the blank sample in freshwater environment at the age of 28 d and 180 d is shown in Figs. 18 and 19, respectively, where 'W' represents fresh water environment and 'FY' represents mixed salt environment.

According to Fig. 18, the pore size distribution trend of concrete in the mixed salt solution is roughly the same as that of the blank sample; with the decrease of pore size, the mercury intrusion content gradually increases, indicating that the proportion of this pore size increases. The most probable aperture of the blank sample and the concrete in mixed salt environments is 28.29 nm and 21.08 nm respectively, and

the mercury intrusion content of the two is 0.114 ml/g and 0.122 ml/g separately, which shows that there is no obvious difference in pore size between the two samples at 28 d age, and the most probable aperture of concrete in mixed salt environment is slightly smaller than that of blank sample. It can be seen from Fig. 19 that when the age increases to 180 d, for the blank sample, the most probable aperture is 40.31 nm, and the content of mercury intrusion is 0.116 ml/g, while for the concrete in mixed salt environment, the most probable pore aperture is 26.27 nm, and the content of mercury intrusion is 0.106 ml/g. The mercury intrusion content of the two is similar, and the pore size distribution of the latter is slightly better than that of the former.

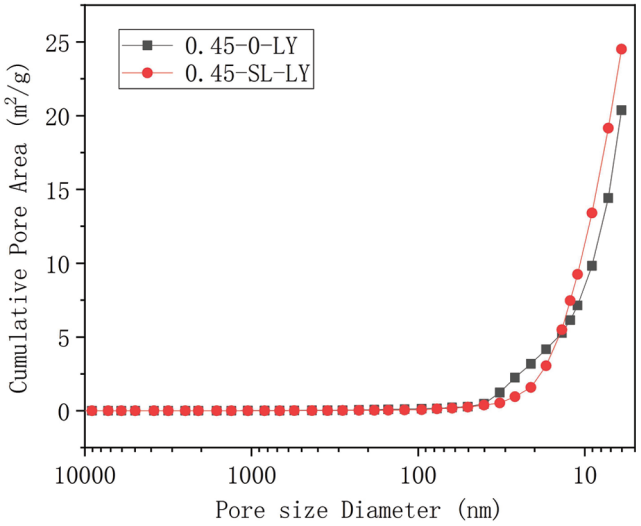


**Figure 17:** Cumulative pore area of concrete at 180 d

**Table 8:** MIP analysis of underwater non-dispersive concrete

| Sample | Age | Total intrusion volume (mL/g) | Median volume pore diameter (nm) | Median area pore diameter (nm) | Average pore diameter (nm) | Porosity (%) |
|---|---|---|---|---|---|---|
| 0.45-0-LY | 28 d | 0.0855 | 28.7 | 11.3 | 19.9 | 19.29 |
| 0.45-SL-LY | 28 d | 0.0794 | 27.5 | 10.2 | 19.2 | 19.06 |
| 0.45-0-LY | 180 d | 0.0874 | 28.1 | 9.8 | 19.2 | 18.64 |
| 0.45-SL-LY | 180 d | 0.0860 | 13.8 | 9.5 | 14.0 | 17.98 |

At 28 d, the cumulative pore area and mercury intrusion trend of concrete under mixed salt environment and the blank sample is shown in Fig. 20, which at 180 d is shown in Fig. 21. The MIP analysis of the two samples is given in Tab. 9. It can be seen from Fig. 20 that at the age of 28 d, the cumulative pore area of concrete in freshwater environment and in mixed salt environment is not significantly different, which is 16.61 $m^2/g$ and 18.76 $m^2/g$ respectively. And from Fig. 21, at the age of 180 d, the cumulative pore area of concrete in the mixed salt environment is higher than that of the blank sample, which is 18.58 $m^2/g$ and 14.45 $m^2/g$ respectively, and the difference is 28.58% compared with the blank sample. In addition, the number of harmful holes of concrete in the mixed salt environment is higher than that in the blank sample. According to Tab. 9, with the increase of age, the porosity of concrete gradually decreases, and the compactness of concrete increases at the same time, which can enhance the impermeability of concrete from macroscopic view. Besides, the porosity of concrete in mixed salt environment is 1.30%

lower than that of blank sample at 28 d, and 3.74% higher than that of blank sample at 180 d. Therefore, the mixed salt environment will increase the porosity of concrete on the whole, which cause the growth in the number of harmful holes, and reduce the impermeability of concrete macroscopically.

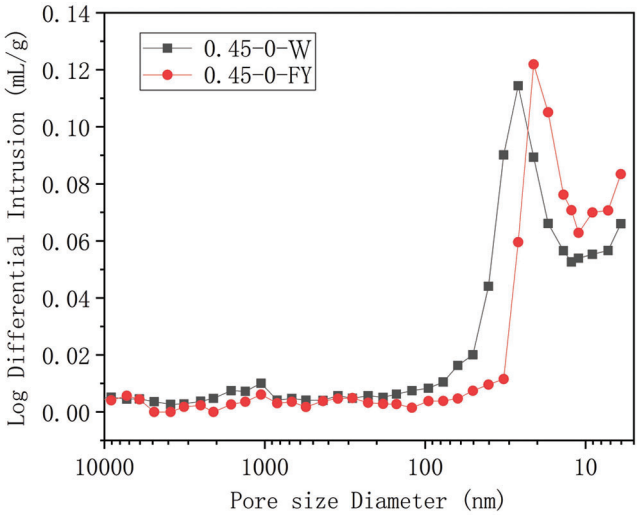


**Figure 18:** Log differential intrusion of concrete at 28 d

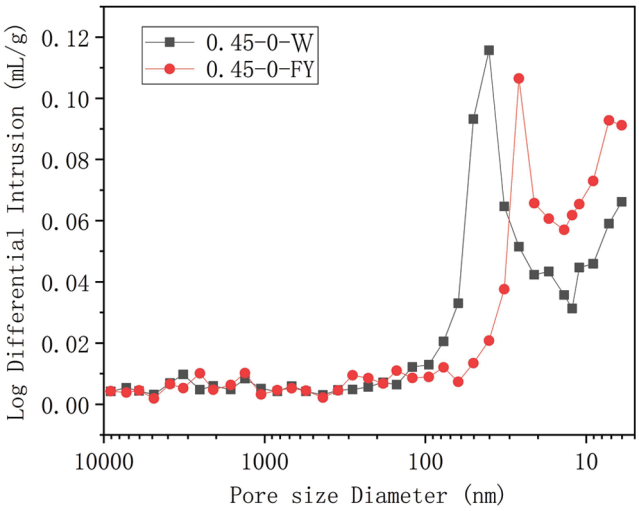


**Figure 19:** Log differential intrusion of concrete at 180 d

*3.3.2 Effect of Slag Powder on Pore Structure of Non-Dispersible Underwater Concrete*

Under mixed salt environment, the pore size distribution of concrete with 60% slag powder and the blank sample at 28 d is shown in Fig. 22, and that of the two at 180 d is given in Fig. 23. As can be seen from Fig. 22, at the age of 28 days, the most probable aperture of the former is smaller than that of the latter-one is 6.03 nm and the other is 21.08 nm; the mercury intrusion content of the two is 0.119 ml/g and 0.122 ml/g respectively. From Fig. 23, when the age of concrete increases to 180 d, the most probable aperture of concrete mixed with slag powder is also smaller than that of the blank sample, which is 7.24 nm and 26.27 nm respectively, and the mercury intrusion of them is 0.128 ml/g and

0.106 ml/g separately. The results demonstrate that the pore size of non-dispersible underwater concrete with slag powder is smaller than that of the blank sample on the whole. That is to say, by adding slag powder, the pore size distribution of concrete can be improved, and the concrete can be more dense, and the impermeability of concrete can be improved macroscopically.

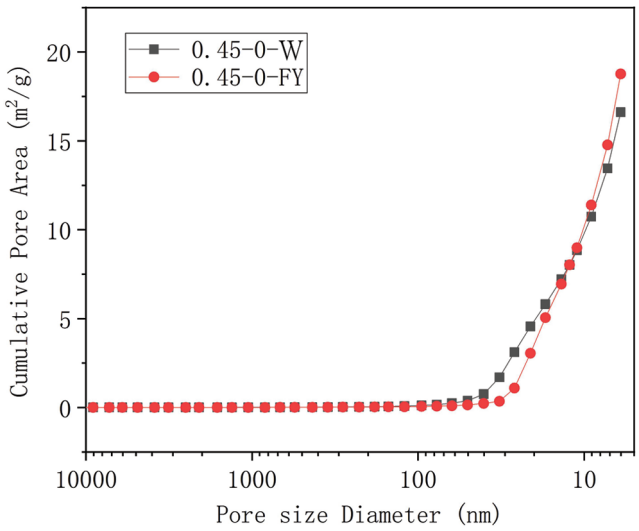


**Figure 20:** Cumulative pore area of concrete at 28 d

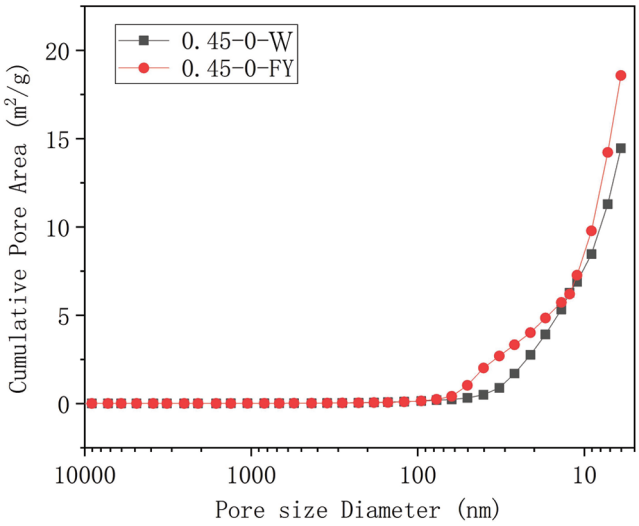


**Figure 21:** Cumulative pore area of concrete at 180 d

Fig. 24 shows the cumulative pore area and mercury intrusion trend of concrete mixed with slag powder and the blank sample at 28 d under mixed salt environment and Tab. 10 displays the MIP analysis of them. It can be seen from Fig. 24 that at the age of 28 d, the cumulative pore area of concrete mixed with slag powder is slightly higher than that of blank sample, while the number of pores with pore size over 20 nm in the former is less than that in the latter. According to Tab. 10, the porosity of concrete mixed with slag

powder is 8.20% lower than that of blank sample at the age of 180 d, which signifies that the porosity of non-dispersible underwater concrete can be reduced by adding slag powder.

**Table 9:** MIP analysis of underwater non-dispersive concrete

| Sample | Age | Total intrusion volume (mL/g) | Median volume pore diameter (nm) | Median area pore diameter (nm) | Average pore diameter (nm) | Porosity (%) |
|---|---|---|---|---|---|---|
| 0.45-0-W | 28 d | 0.0918 | 29.1 | 11.8 | 21.5 | 20.04 |
| 0.45-0-FY | 28 d | 0.0826 | 26.5 | 10.7 | 20.6 | 19.78 |
| 0.45-0-W | 180 d | 0.0876 | 31.1 | 10.5 | 20.2 | 18.46 |
| 0.45-0-FY | 180 d | 0.0825 | 28.4 | 20.3 | 20.8 | 19.15 |

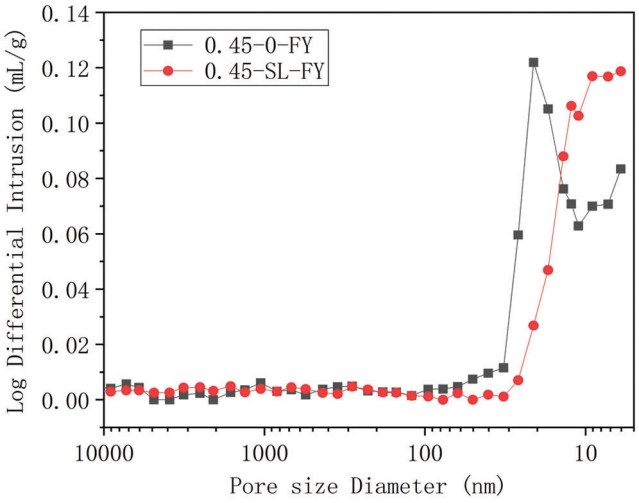


**Figure 22:** Log differential intrusion of concrete at 28 d

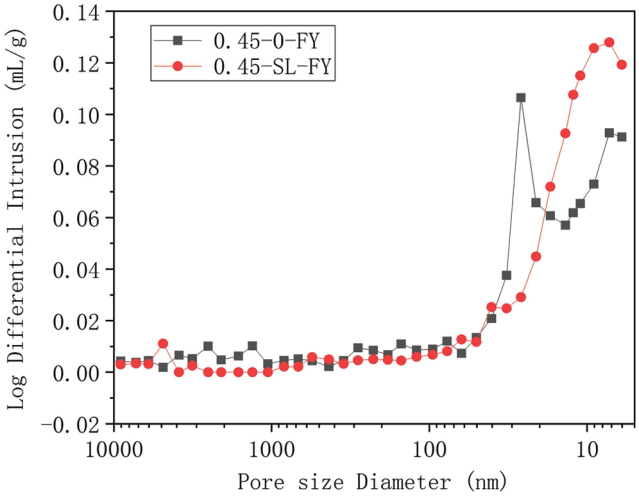


**Figure 23:** Log differential intrusion of concrete at 180 d

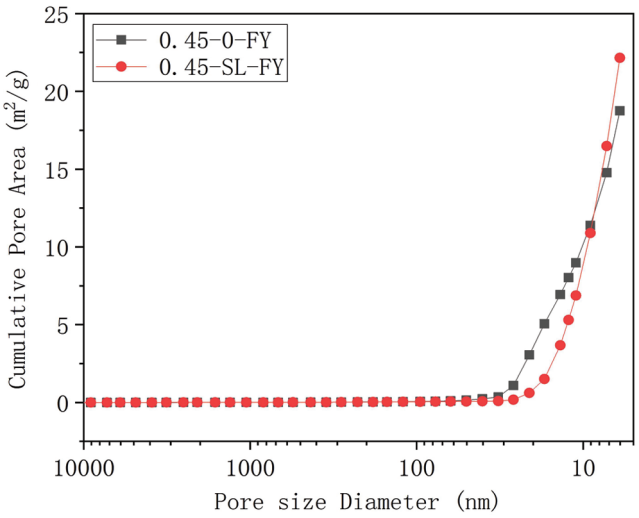


**Figure 24:** Cumulative pore area of concrete at 28 d

**Table 10:** MIP analysis of underwater non-dispersive concrete

| Sample | Age | Total intrusion volume (mL/g) | Median volume pore diameter (nm) | Median area pore diameter (nm) | Average pore diameter (nm) | Porosity (%) |
|---|---|---|---|---|---|---|
| 0.45-0-FY | 28 d | 0.0826 | 26.5 | 10.7 | 20.6 | 19.78 |
| 0.45-SL-FY | 28 d | 0.0746 | 22.7 | 9.0 | 19.5 | 18.61 |
| 0.45-0-FY | 180 d | 0.0825 | 28.4 | 20.3 | 20.8 | 19.15 |
| 0.45-SL-FY | 180 d | 0.0892 | 24.2 | 9.3 | 18.3 | 17.58 |

## 4 Conclusions

In this paper, the pore structure characteristics of non-dispersible underwater concrete were investigated, and the pore size distribution, porosity and pore structure characteristics of concrete were compared and analyzed. The conclusions are as follows:

1. In the environment of fresh water and salt solution, the porosity of non-dispersible underwater concrete decreases with the increase of age. This is because the hydration reaction of cement in concrete continues, which not only improves the compactness of concrete, but also enhances its impermeability.
2. The pore size distribution of concrete in fresh water environment is better than that in both sulfate environment and mixed salt environment. This means that sulfate and mixed salt are not conducive to the development of pore structure of non-dispersible underwater concrete, which may lead to the decrease of concrete impermeability on the macro level. Furthermore, chloride salt has little effect on the pore structure of non-dispersible underwater concrete.
3. The addition of slag powder improves the pore size distribution of non-dispersible underwater concrete, cause the reduction of the porosity, and makes the concrete structure more compact, which improves the impermeability of concrete macroscopically.

**Funding Statement:** This work is supported by the National Natural Science Foundation of China (51878116 and 51902270); Liaoning Province Key Project of Research and Development Plan (2020JH2/

10100016); Dalian Science and Technology Innovation Fund Project (2020JJ26SN060); the Open Research Fund of State Key Laboratory of Simulation and Regulation of Water Cycle in River Basins (China Institute of Water Resources and Hydropower Research), Grant No. IWHR-SKL-201910.

**Conflicts of Interest:** The authors declare that they have no conflicts of interest to report regarding the present study.

## References

1. Tveit, P. (2000). Ideas on downward arched and other underwater concrete tunnels. *Tunnelling and Underground Space Technology, 15(1),* 69–78. DOI 10.1016/S0886-7798(00)00031-6.
2. Ye, K. (2016). *Research on high performance marine underwater concrete (Master's Thesis)*. Yangzhou University, China.
3. China National Petroleum Corporation (2003). Technical Code for construction of underwater non-dispersible concrete. Enterprise Standard of China National Petroleum Corporation, Q/CNPC92−2003.
4. Yao, S. X. Jr, Gerwick, B. C. (2004). Underwater concrete. *Concrete International, 26(1),* 79–83.
5. Mazhoud, B., Perrot, A., Picandet, V., Rangeard, D., Courteille, E. (2019). Underwater 3D printing of cement-based mortar. *Construction and Building Materials, 214,* 458–467. DOI 10.1016/j.conbuildmat.2019.04.134.
6. Wu, S., Jiang, S. F., Shen, S., Wu, Z. (2019). The mix ratio study of self-stressed anti-washout underwater concrete used in nondrainage strengthening. *Materials, 12(2),* 324. DOI 10.3390/ma12020324.
7. Zhong, W. Q., Zhang, Q. L., Zhang, S. W. (2008). Development and application of non-dispersible underwater concrete. *Journal of Building Structures, 29(S1),* 146–151 (In Chinese).
8. Liu, M. L., Du, B. L., He, D. L., Song, J. C., Luo, X. Y. et al. (2017). Effect of different flocculants on non-dispersible underwater concrete. *Guangdong Building Materials, 33(04),* 48–50 (In Chinese).
9. Falkner, H., Henke, V. (1998). Application of steel fibre concrete for underwater concrete slabs. *Cement and Concrete Composites, 20(5),* 377–385. DOI 10.1016/S0958-9465(98)00005-5.
10. Zhong, W. Q., Zhang, Z. W. (2009). The performance of non-dispersible underwater concrete and its effect factors. *China Water Transport, 9(07),* 263–264 (In Chinese).
11. Assaad, J. J., Issa, C. A. (2013). Mechanisms of strength loss in underwater concrete. *Materials and Structures, 46 (10),* 1613–1629. DOI 10.1617/s11527-012-0004-2.
12. Grzeszczyk, S., Jurowski, K., Bosowska, K., Grzymek, M. (2019). The role of nanoparticles in decreased washout of underwater concrete. *Construction and Building Materials, 203,* 670–678. DOI 10.1016/j.conbuildmat.2019.01.118.
13. Sikandar, M. A., Ahmad, W., Khan, A. (2020). Effect of various anti-washout admixtures on the properties of non-dispersible underwater concrete. *Construction and Building Materials, 245,* 118469. DOI 10.1016/j.conbuildmat.2020.118469.
14. Liu, L. X. (2001). Brief introduction on the study of erosion and prevention of concrete in salt lake and saline soil area of Chaerhan, Chaidamu. *Journal of Building Materials, 4(4),* 395–400.
15. Zhao, J., Zhu, Z. P., Wu, H. J. (2017). Durability study of non-dispersion underwater concrete in sea water environment. *Journal of Dalian Jiaotong University, 38(1),* 86–89 (In Chinese).
16. Gu, L. N., Zhao, J., Yang, F., Liu, S. T. (2018). Structure and performance of non-dispersion underwater concrete in marine environment. *Journal of Dalian Jiaotong University, 39(03),* 104–108 (In Chinese).
17. Qiao, D., Xia, W. J., Zhao, Y., Zhou, X., Xu, Y. F. (2010). Durability of concrete in saline soil in Lianyungang. *Chinese Journal of Geotechnical Engineering, 32(S2),* 611–614.
18. Qiao, H. X., Gong, W., Cheng, Q. Y., Dong, J. M., Chen, G. F. et al. (2015). Durability of magnesium cement reinforced concrete in saline soil area. *Journal of China Coal Society, 40(S2),* 346–352.
19. Jiang, W. D., Chen, X., Yan, J., Liu, B. (2008). Durability of the corrosion-resistant concrete in saline soil area. *Journal of Northeastern University, 29(2),* 280–283.
20. Fujiwara, Y., Maruya, T., Owaki, E. (1992). Degradation of concrete buried in soil with saline ground water. *Nuclear Engineering & Design, 138(2),* 143–150. DOI 10.1016/0029-5493(92)90289-8.

21. Lin, D., Yi, B., Chen, Y., Zhang, J., Hong, Y. (2014). Research development of the corrosion of reinforced concrete in saline soil environment. *Materials Review, 28(6),* 137–141.
22. Xue, H., Shen, X., Wang, R., Liu, Q., Liu, Z. et al. (2017). Mechanism analysis of chloride resistance of aeolian sand concrete under wind-sand erosion and dry-wet circulation. *Transactions of the Chinese Society of Agricultural Engineering, 33(18),* 118–126.
23. Yu, W., Li, L. Y., Page, C. L. (2005). Modelling of chloride ingress into concrete from a saline environment. *Building and Environment, 40(12),* 1573–1582. DOI 10.1016/j.buildenv.2005.02.001.
24. Wang, Y. Z., Cheng, Y., Zhou, C., Yang, J. G. (2017). Experimental study on the strength of chloride saline soil subgrade in western china treated by stabilizing method. *China Building Materials Science & Technology, 26(2),* 63–65. (In Chinese).
25. Zhang, J., Bai, P. C., Yan, C. W., Liu, S. G. (2016). Study on chloride binding capacity of concrete in west chlorine saline soil region. *China Concrete and Cement Products, 4,* 21–24 (In Chinese).
26. Yan, C. W., Li, J., Zhang, J., Liu, S. G. (2016). Chloride diffusion in concrete in a west chlorine saline soil medium. *Journal of Functional Materials, 47(2),* 2060–2066 (In Chinese).
27. Cui, S. A., Ye, Y. Z., Fu, F., Liu, Z. F. (2010). Study on resistance to chloride ion penetration of high performance concrete for high speed railway bridge pile. *Advanced Materials Research, 150−151,* 542–546. DOI 10.4028/www.scientific.net/AMR.150-151.542.
28. State Economic and Trade Commission of China (2000). Test code on non-dispersible underwater concrete. China Electric Power Industry Standard, DL/T5117−2000.